Available online at www.sciencedirect.com
ScienceDirect
Applied Catalysis B: Environmental 83 (2008) 46–55
APPLIED CATALYSIS B: ENVIRONMENTAL
www.elsevier.com/locate/apcatb

Homogeneus ferrioxalate-assisted solar photo-Fenton degradation of Orange II aqueous solutions

J.M. Monteagudo *, A. Durán, C. López-Almodóvar

Universidad de Castilla-La Mancha, Departamento de Ingeniería Química, Escuela Técnica Superior de Ingenieros Industriales, Avda, Camilo José Cela, 1, 13071 Ciudad Real, Spain

Received 12 December 2007; received in revised form 29 January 2008; accepted 4 February 2008
Available online 9 February 2008

Abstract

The decoloration and mineralization of the non-biodegradable azo dye Orange II (OII) solutions by solar photo-Fenton (SPF) and ferrioxalate-assisted solar photo-Fenton (SPFox) reactions have been carried out in a solar compound parabolic collector (CPC). A comparative study of these two processes was done by using multivariate experimental design including the following variables: pH and initial concentrations of Fe(II), oxalic acid, H_2O_2 and OII. The efficiency of photocatalytic degradation was determined from the analysis of the following parameters: color, total organic carbon (TOC) and chemical oxygen demand (COD). The decoloration rate pseudoconstant was calculated as a function of the accumulated solar energy received by the water solution. Experimental data were fitted using neural networks (NNs) which reproduce the results within 85% of confidence and allow the simulation of the process for any value of variables in the experimental range studied. The results reveal that the addition of oxalic acid to the Fenton system (Fe(II)/H_2O_2) irradiated under sunlight improves the photocatalytic efficiency since ferrioxalate complexes absorb strongly and a higher portion of the solar spectrum can be used. In addition, the SPFox system permits the use of an iron concentration below the discharge legal limit (2 ppm) and oxalic acid can be used to pH adjustment, reducing the operation costs of Fe removal and chemicals. Under the optimal conditions, 100% decoloration of dye solution can be reached by using both processes, but with different accumulated solar energy (SPF system: 34 W h, SPFox system: 16 W h). However, the efficiency of TOC and COD removal was higher in the SPFox process (80% TOC and 100% COD removal in SPFox system versus 50% TOC and 80% COD removal in SPF system).

Keywords: Orange II; Ferrioxalate; Photo-Fenton; Neural networks; CPC

1. Introduction

Pollution of water by synthetic dyes generated from the textile industry is a serious problem in the developed countries. The large degree of aromatics present in dye molecules and the stability of new dyes prevent mineralization of these compounds by conventional aerobic biological treatment processes and contribute notably to the toxicity of the effluents [1–3].

Physical or chemical operations for the removal of dye pollutants, such us adsorption, chemical flocculation, electro-flotation, reverse osmosis, ultrafiltration, coagulation or ion exchange have been used efficiently [4] although they are non-destructive, since they just transfer dissolved organic contaminants from wastewater phase to another phase that will have to be regenerated and post-treated by expensive operations [5]. Hence, there is considerable current interest in developing alternative and more cost-effective techniques.

For that reasons, advanced oxidation processes (AOPs) have emerged as an important class of technologies for the oxidation of dyes into CO_2, H_2O and inorganic ions, or biodegradable compounds [6]. Among AOPs, homogeneus Fenton reaction (system Fe(II)/H_2O_2) is one of the most important processes to generate hydroxyl radicals, $^{\bullet}OH$ [7]. Besides, it is well known that when Fenton's reagent is combined with UV–visible irradiation (photo-Fenton system), the efficiency of degradation is considerably improved due to the continuous regeneration of Fe^{2+} via photoreduction of Fe^{3+} and extra generation of new $^{\bullet}OH$ radicals with H_2O_2 [8].

However, the production of photons with artificial ultraviolet light sources requires an important electrical energy demand [9]. As alternative to UV lamps, solar technology can be used to

* Corresponding author. Fax: +34 926 295361.
E-mail address: josemaria.monteagudo@uclm.es (J.M. Monteagudo).

0926-3373/$ – see front matter © 2008 Elsevier B.V. All rights reserved.
doi:10.1016/j.apcatb.2008.02.002

reduce the degradation process costs. Thus, the photochemical degradation of contaminants using sunlight has been successfully used being an economically viable process since solar energy is an abundant natural energy source and can be used instead of artificial light sources which are costly and hazardous [10–14].

Nevertheless, H_2O_2 has a low molar extinction coefficient, and so it only uses photons that represent minority of total solar radiation, below 350–400 nm, around 3% of solar irradiation [15]. Ferrioxalate is a photosensitive complex that is able to expand the usage of solar spectrum range up to 450 nm (≈18 % of solar irradiation) improving the oxidation efficiency of the solar-Fenton process [6,16,17]. Besides, ferrioxalate photochemistry provides extra sources of oxidant H_2O_2 and catalyst Fe^{2+} for the Fenton reaction to yield more $^{\bullet}OH$ radicals [18–21] according to the following reactions:

$$[Fe(C_2O_4)_3]^{3-} + h\nu \rightarrow Fe^{2+} + 2C_2O_4^{2-} + C_2O_4^{\bullet -} \quad (1)$$

$$C_2O_4^{\bullet -} + [Fe(C_2O_4)_3]^{3-} \rightarrow Fe^{2+} + 3C_2O_4^{2-} + 2CO_2 \quad (2)$$

$$C_2O_4^{\bullet -} + O_2 \rightarrow 2CO_2 + O_2^{-} \quad (3)$$

$$O_2^{-} + H^{+} \rightarrow HO_2^{\bullet} \quad (4)$$

$$HO_2^{\bullet} + HO_2^{\bullet} \rightarrow H_2O_2 + O_2 \quad (5)$$

$$H_2O_2 + Fe^{2+} \rightarrow Fe^{3+} + {}^{\bullet}OH + OH^{-} \quad (6)$$

In recent years, ferrioxalate has been widely used in the photo-Fenton reaction involving ferric compounds, but there is very little information on the ferrioxalate-assisted photo-Fenton systems using ferrous initiated processes.

In the present work, we have studied the degradation of Orange II solutions ($C_{16}H_{11}N_2NaO_4S$, see Fig. 1) appearing in the manufacturing wastewaters of dyeing of textiles, using a solar photo-Fenton system, and a ferrioxalate-assisted solar photo-Fenton system. The degradation of Orange II has already been studied by using several treatment processes including electrocoagulation [22], photo-Fenton reactions induced by natural sunlight [23], or activated by heterogeneous supported Fe catalyst on Nafion/Glass fibers [24], bentonite clay [25], Fe/C and Fe/Nafion/C catalyst [14], pillared bentonite [26], saponite clay [27], using a carbon/Fe catalyst [28], and a novel composite of iron oxide and silicate [29]. The reductive degradation of Orange II in aqueous solution to sodium sulfanilate [30] and a reduction and photo-oxidation process [31] were also reported. Finally, photocatalytic oxidation in the presence of TiO_2 has been used to oxidise Orange II present in aqueous solutions by using artificial ultraviolet light sources [32–34] and under solar irradiation by using compound parabolic collectors [35]. However, the degradation of Orange II solutions under solar photo-Fenton processes using ferrioxalate in a CPC reactor has not been reported up to date.

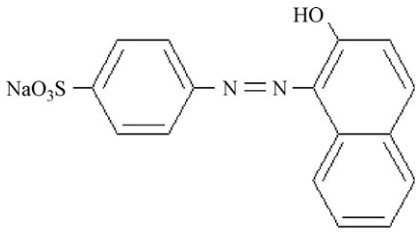

Molecular Weight: 350.32 g/mol
λ_{max}(chromophore)= 486 nm
λ_{max}(naphthalene)= 310 nm
λ_{max}(benzene)= 228 nm

Fig. 1. Chemical structure of reactive Orange II.

The objective of this research is the study of effect of oxalic acid on the homogeneus solar photo-Fenton degradation of Orange II solutions and to analyze the viability of using low iron concentrations (below discharge limit according to the European Union Directive) to avoid the ulterior Fe removal process thus reducing operation costs. We have also compared the photocatalytic efficiencies of the two systems solar photo-Fenton (Fe^{2+}/H_2O_2/solar) and ferrioxalate-assisted solar-photo-Fenton (Fe^{2+}/oxalic acid/H_2O_2/solar). The use of ferrous sulphate is advantageous since it is less corrosive than ferric salts, very cheap and more soluble than ferric compounds.

To determine the optimal values of experimental variables for color removal and mineralization of dye solutions, a multivariate experimental design was performed according to the methodology of response surface [36]. The influence of pH and initial concentrations of Orange II, hydrogen peroxide, Fe(II) and oxalic acid on the degradation process was investigated. Results of experimental tests were fitted using neural networks, NNs [37–39], which allows the values of kinetic degradation rate constants (response function) to be estimated within the studied range as a function of process factors. The decrease of color and TOC and COD content was monitored.

2. Experimental

2.1. Materials

Orange II solutions were prepared dissolving Orange II (Aldrich, disodium salt, dye content 85%) in distilled water, without further purification. $FeSO_4 \cdot 7H_2O$ (Panreac, analytical grade) and $H_2C_2O_4 \cdot 2H_2O$ (Panreac, 99.5 %) were added to the wastewater to form ferrioxalate complexes to be used in situ immediately because of its light sensitivity. Commercial hydrogen peroxide (30%, w/v, Merck) was added to the Orange II solutions at the beginning of the reaction after addition of Fe(II) and oxalic acid and pH adjustment. 0.1 M H_2SO_4 and 6 M NaOH solutions were used to pH adjustment of the dye solutions prior to degradation.

2.2. Irradiation experiments

The decoloration and mineralization of the dye solutions was carried out by using solar light. The experimental setup (Fig. 2) based on a previous study [40] shows the solar reactor (50 L) that consists of a continuously stirred tank, a centrifugal recirculation pump, an solar collector unit with an area of 2 m^2 (concentration factor = 1) in an aluminium frame mounted on a fixed south-facing platform tilted 45° in Ciudad Real (Spain) and connecting

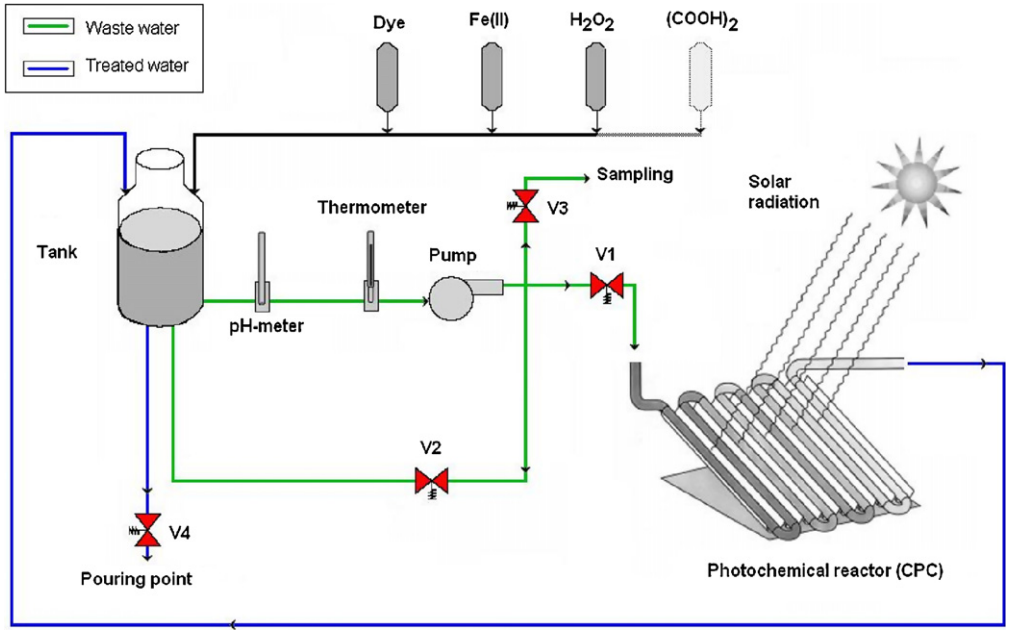

Fig. 2. Experimental set-up based on a compound parabolic solar reactor.

tubing and valves. This solar unit has 16 borosilicate-glass tubes (OD 32 mm, transmissivity >50% at $\lambda > 300$ nm; >75% at $\lambda > 320$ nm; >90% at (> 350 nm) connected by plastic joints, and the total illuminated volume inside the absorber tubes is 16 L. Solar ultraviolet radiation was measured by a global UV radiometer Ecosystem model ACADUS 85 tilted 45° which provide data in terms of incident solar power, W m^{-2}, and accumulated solar energy, W h. All photocatalytic experiments were carried out under solar illumination on sunny days of February to May 2007, between 12 a.m. and 4 p.m.

2.3. Analysis

Changes in the Orange II concentration were determined from the absorbance at 480 nm using a UV–vis spectrophotometer (Zuzi 4418PC). chemical oxygen demand (COD) was measured according to an EPA approved reactor digestion method (COD range of 0–150 mg/L) using a HACH DR2000. The degree of mineralization was followed by TOC variation. TOC was determined using a TOC-5050 Shimazdu analyser. H_2O_2 in solution was determined by titration through an aqueous solution of potassium permanganate (0.02 M) using an automatic Titrino SET/MET 702 (Metrohm). Nitrates and sulphates released from the degradation of OII were determined using a Metrohm ion chromatograph fitted with a 732 IC Conductivity Detector.

2.4. Experimental design

The central composite experimental design was applied to investigate the effect of different variables for each process (Table 1):

(a) Solar photo-Fenton: pH and initial concentrations of Fe(II), H_2O_2 and Orange II.
(b) Ferrioxalate-assisted solar photo-Fenton: pH and initial concentrations of Fe(II), H_2O_2 and oxalic acid.

Each design consists of three series of experiments:

(i) a factorial design 2^k (all possible combinations of codified values + 1 and −1) which in the case of $k = 4$ variables consists of 16 experiments;
(ii) axial of star points (codified values $\alpha = 2^{k/4} = \pm 2.378$) consisting of $2^k = 8$ experiments, and
(iii) central, replicates of the central point (4 experiments)

The temperature was not controlled during the experiment, but it was measured during reaction, so that the average temperature was included in the fitting. It was found that the initial rate of decoloration of Orange II obeys pseudo-first order kinetics. The values of k_d (decoloration rate pseudoconstant, $W^{-1}\,h^{-1}$) were related to the accumulated solar energy received by the water solution.

3. Results and discussion

3.1. Decoloration of dye solutions

As previously reported by the authors [41], Orange II degradation due to H_2O_2 alone or direct photolysis is almost negligible. However, the irradiation of dye solutions with solar light in the presence of the heterogeneous catalyst TiO_2-P-25 with addition of hydrogen peroxide caused 100 % decoloration after 30 min and 90% TOC removal in 180 min. Nevertheless, at industrial scale, the use of an homogeneus catalyst such us Fe(II) could offer an economical and practical alternative for the destruction of this environmental contaminant if a ferrous concentration below discharge legal limit (2 ppm) can be used efficiently. The removal or treatment of the sludge of treated

Table 1
The 4-factor central composite design matrix and the values of the response function (k_d)

Solar photo-Fenton system						Ferrioxalate-assisted solar photo-Fenton system, [dye] = 25 ppm				
Experimets	$[H_2O_2]$ (ppm)	$[FeSO_4]$ (ppm)	pH	[dye] ppm	k_d (W^{-1} h^{-1})	$[H_2O_2]$ (ppm)	$[FeSO_4]$ (ppm)	pH	$[H_2C_2O_4]$ (ppm)	k_d (W^{-1} h^{-1})
1	450	6	6.5	25	0.031	337.5	6	3.88	45	0.270
2	150	6	6.5	25	0.037	112.5	6	3.88	45	0.269
3	450	2	6.5	25	0.004	337.5	2	3.88	45	0.130
4	150	2	6.5	25	0.002	112.5	2	3.88	45	0.255
5	450	6	3.5	25	0.079	337.5	6	2.63	45	0.291
6	150	6	3.5	25	0.087	112.5	6	2.63	45	0.279
7	450	2	3.5	25	0.112	337.5	2	2.63	45	0.114
8	150	2	3.5	25	0.115	112.5	2	2.63	45	0.184
9	450	6	6.5	15	0.026	337.5	6	3.88	15	0.370
10	150	6	6.5	15	0.010	112.5	6	3.88	15	0.340
11	450	2	6.5	15	0.029	337.5	2	3.88	15	0.334
12	150	2	3.5	15	0.008	112.5	2	3.88	15	0.207
13	450	6	3.5	15	0.089	337.5	6	2.63	15	0.245
14	150	6	3.5	15	0.078	112.5	6	2.63	15	0.274
15	450	2	3.5	15	0.184	337.5	2	2.63	15	0.141
16	150	2	3.5	15	0.026	112.5	2	2.63	15	0.239
17	600	4	5	20	0.064	450	4	3.25	30	0.317
18	0	4	5	20	0.002	0	4	3.25	30	0.050
19	300	8	5	20	0.059	225	8	3.25	30	0.457
20	300	0	5	20	0.019	225	0	3.25	30	0.186
21	300	4	8	20	0.010	225	4	4.5	30	0.223
22	300	4	2	20	0.049	225	4	2	30	0.085
23	300	4	5	30	0.085	225	4	3.25	60	0.219
24	300	4	5	10	0.055	225	4	3.25	0	0.333
25	300	4	5	20	0.067	225	4	3.25	30	0.260
26	300	4	5	20	0.064	225	4	3.25	30	0.227
27	300	4	5	20	0.069	225	4	3.25	30	0.266
28	300	4	5	20	0.070	225	4	3.25	30	0.268
Codified levels										
(+α)	600	8	8	30		450	8	4.5	60	
(−α)	0	0	2	10		0	0	2	0	
(+1)	450	6	6.5	25		337.50	6.00	3.88	45.00	
(−1)	150	2	3.5	15		112.50	2.00	2.63	15.00	
(0)	300	4	5	20		225	4	3.25	30	
Additional experiments										
29	900	8	2.5	25	0.159	225	18	3.25	30	0.446
30	750	8	2.5	25	0.144	225	18	3.25	15	0.440
31	–	–	–	–	–	225	13	3.25	30	0.394
32	–	–	–	–	–	225	13	3.25	15	0.315
33	–	–	–	–	–	225	18	3.25	7	0.296

Solar photo-Fenton and Ferrioxalate-assisted solar photo-Fenton systems.

wastewater containing Fe ions is expensive and the use of chemicals and manpower would be necessary [14,42].

To achieve this goal using a maximum concentration of 2 ppm Fe^{2+} (limit value in treated water to be dumped directly into the environment, according to the European Union Directive [42]), the addition of oxalic acid to the water to form oxalate complexes was investigated.

In all the solar photo-Fenton experiments (with or without ferrioxalate), the disappearance of Orange II followed pseudo-first order kinetics with respect to the dye concentration as follows:

$$r = -\frac{dC}{di} = k_d C \tag{7}$$

where "r" is the reaction rate, "C" is the concentration (mg/L) of Orange II at an accumulated solar energy "i" (W h) and "k_d" is the pseudo-first order decoloration kinetic rate constant (W^{-1} h^{-1}) for the photochemical reaction. This equation can be integrated between $i = 0$ and $i = i$, yielding:

$$\ln \frac{Co}{C} = k_d i \tag{8}$$

where Co is the initial concentration of Orange II. According to this expression, a plot of the first term versus "i" must yield a straight line validating Eq. (8) whose slope is k_d.

To study the effect of pH and initial concentration of Orange II, hydrogen peroxide, Fe(II) and oxalic acid on response function (kinetic decoloration rate constant), a central

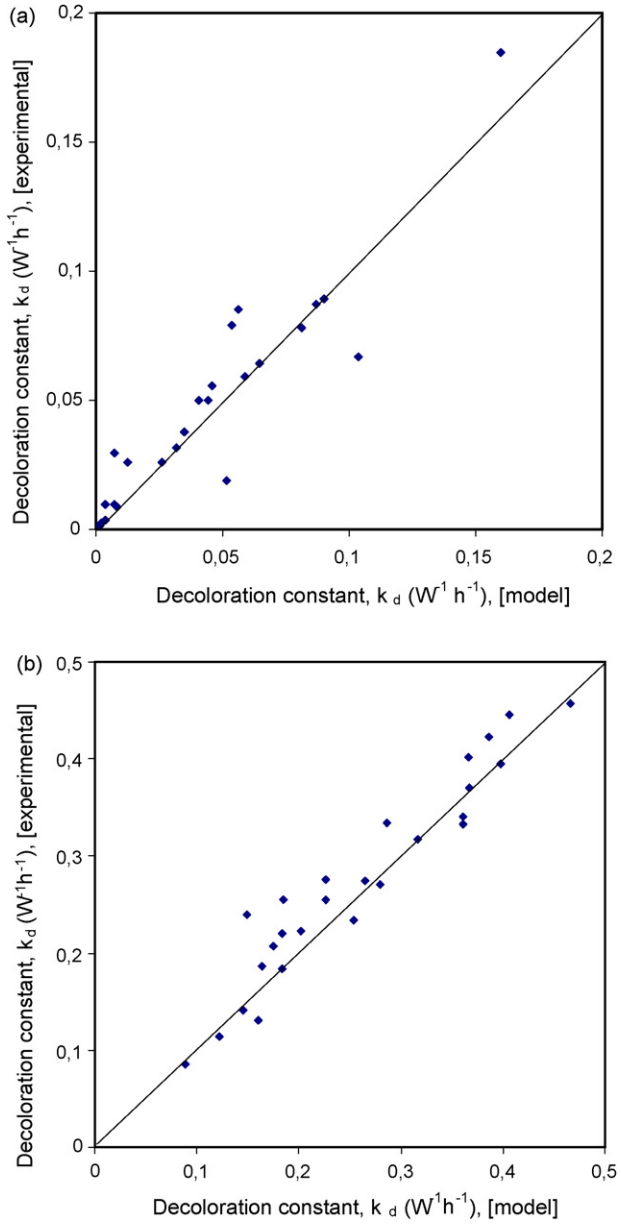

Fig. 3. Neural network fittings of the decoloration rate pseudoconstant. (a) Solar photo-Fenton process; (b) Ferrioxalate-assisted solar photo-Fenton.

composite design for each system (SPF or SPFox) was performed. The central composite design matrix (Table 1) shows the operation conditions (factors values) and the k_d values obtained. The temperature was not controlled during the experiment, but it was measured during reaction, so that the average temperature was included in the fitting. In all experiments, the temperature varied between 20 and 29 °C. Experimental results and NNs fittings of these constants are shown in Fig. 3 and are in good agreement, with an average error lower than 16% for dye decoloration. The equations and parameters for the fitting of k_d using NNs are shown in Table 2. N_1 and N_2 are general factors related to the first and the second neuron, respectively. W_{11} W_{15} are the contribution parameters to the first neuron and represent the influence of each of the five factors in the process. W_{21} to W_{25} are the contributions to the second neuron and are related to the same factors. From these results it is possible to deduce the effect of each parameter on the response function.

The results of a saliency analysis on the input variables for each neural network (%) are shown in Table 3. It is confirmed that pH and initial concentration of hydrogen peroxide are the most significant factors affecting the decoloration kinetics of solar photo-Fenton process whereas the initial concentration of oxalic acid, Fe(II) and H_2O_2 are the most significant variables affecting the ferrioxalate-asssisted solar photo-Fenton process, as will be explained below.

3.1.1. Effect of initial concentrations of Fe(II), H_2O_2 and oxalic acid

The equations shown in Table 2 allow a simulation analysis of the effect of any of the studied variables on the value of k_d. For example, the influence of the initial concentration of H_2O_2 and Fe(II) is represented in three dimensions in Fig. 4.

Solar photo-Fenton process results (Fig. 4a) show that k_d increases with initial Fe(II) concentration over the range studied until reaching a maximum value ($k_d = 0.20\ W^{-1}\ h^{-1}$) when a low concentration of H_2O_2 is used ($\leq$450 ppm). This fact indicates that Fe^{2+} can significantly accelerate the decomposition of H_2O_2 to form more hydroxyl radicals. Above this hydrogen peroxide optimal concentration, the decoloration of Orange II had no significant change and the effect of Fe(II) is negligible. This can be explained with the kinetic photo-Fenton mechanism shown in Table 4 [39]. It is well known that an increase in H_2O_2 concentration produces a higher amount of $^{\bullet}OH$ radicals (reactions 1 and 18 in Table 4) responsible for Orange II destruction. However, an excess of hydrogen peroxide reduces catalytic activity since it favours reaction 3 (where $^{\bullet}OH$ reacts with peroxide), reducing the amount of radicals available to destroy Orange II and producing the well-known *scavenger effect*. Although other radicals ($HO_2^{\bullet}$) are produced, their oxidation potential is much smaller than that of the hydroxyl radicals. Additionally, decomposition of hydrogen peroxide to form water and oxygen (reactions 3 + 13 + 17) is also favoured.

Fig. 4b and c shows the results obtained in the ferrioxalate-assisted solar photo-Fenton system with different initial oxalic acid concentrations. It can be concluded that higher k_d values were obtained (typically $k_d = 0.3–0.5\ W^{-1}\ h^{-1}$) due to the faster generation of Fe^{2+} ion by photolysis of ferrioxalate and additional hydroxyl radicals produced (Eqs. (1)–(6)). The photolysis of ferrioxalate in the presence of hydrogen peroxide is a continuous source of Fenton's reagent. At a given initial oxalic acid concentration, as initial Fe^{2+} was increased (until an optimal value depending on initial $H_2C_2O_4$ concentration) the optimal $[H_2O_2]/[Fe^{2+}]$ molar ratio decreased possibly due to the increase of H_2O_2 amount in the medium by photolysis of oxalate complexes according to the Eqs. (1)–(5). Above the optimal Fe^{2+} dosage, the decrease in decoloration rate is due to Fe^{2+} competing $^{\bullet}OH$ with dye molecules as it is shown in Eq. (3) of Table 4.

On the other hand, the color removal efficiency increased with the $[H_2C_2O_4]/[Fe]$ molar ratio up to 3, beyond which it

Table 2
Equation and parameters of neural network fittings for orange ii degradation under the processes: solar photo-Fenton and ferrioxalate-assisted solar photo-Fenton

Neural network fitting		
Equation[a]	Solar photo-Fenton system $k_d[W^{-1}\,h^{-1}] = N_1 \times (1/(1 + 1/\mathrm{Exp}([H_2O_2] \times W_{11} + [Fe] \times W_{12} + [pH] \times W_{13} + [\mathrm{OrangeII}] \times W_{14} + [\mathrm{Temperature}] \times W_{15}))) + N_2 \times (1/(1 + 1/\mathrm{Exp}([H_2O_2] \times W_{21} + [Fe] \times W_{22} + [pH] \times W_{23} + [\mathrm{OrangeII}] \times W_{24} + [\mathrm{Temperature}] \times W_{25})))$	
Weight factors	Parameter	Values of neurons and factors to obtain the decoloration kinetic rate constant of dye solutions (k_d)
N_1	Neuron	−1.7835
W_{11}	$[H_2O_2]$	−5.0660
W_{12}	$[FeSO_4]$	−1.5022
W_{13}	[pH]	−4.7215
W_{14}	[Orange II]	−2.5801
W_{15}	[Temperature]	2.1726
N_2	Neuron	0.4721
W_{21}	$[H_2O_2]$	−0.6036
W_{22}	$[FeSO_4]$	−1.5022
W_{23}	[pH]	−5.7534
W_{24}	[Orange II]	−0.6091
W_{25}	[Temperature]	2.5650
Equation[a]	Ferrioxalate-assisted solar photo-Fenton system $k_d[W^{-1}\,h^{-1}] = N_1 \times (1/(1 + 1/\mathrm{Exp}([H_2O_2] \times W_{11} + [Fe] \times W_{12} + [pH] \times W_{13} + [H_2C_2O_4] \times W_{14} + [\mathrm{Temperature}] \times W_{15}))) + N_2 \times (1/(1 + 1/\mathrm{Exp}([H_2O_2] \times W_{21} + [Fe] \times W_{22} + [pH] \times W_{23} + [H_2C_2O_4] \times W_{24} + [\mathrm{Temperature}] \times W_{25})))$	
Weight factors	Parameter	Values of neurons and factors to obtain the decoloration kinetic rate constant of dye solutions (k_d)
N_1	Neuron	0.1846
W_{11}	$[H_2O_2]$	−7.8220
W_{12}	[Fe]	−3.5931
W_{13}	$[H_2C_2O_4]$	7.3931
W_{14}	[Temperature]	0.9612
N_2	Neuron	0
W_{21}	$[H_2O_2]$	0
W_{22}	[Fe]	0.3531
W_{23}	$[H_2C_2O_4]$	19.2936
W_{24}	[Temperature]	0.7504

[a] Parameters values in equations must be previously normalized to the (0.1) interval.

declined, because at an $[H_2C_2O_4]$/[Fe] molar ratio of 3, the Fe(III) ions were complexed with the maximum amount of oxalate, in the form of the saturated complex $Fe(C_2O_4)_3^{3-}$ (ferric complexed with three oxalate molecules as its limit load). As it can be seen in Fig. 4b and c, the optimal $[H_2C_2O_4]$/[Fe] molar ratio is 10 ppm $H_2C_2O_4$/5 ppm Fe $<>$ 0.097 mM $H_2C_2O_4$/0.027 mM Fe (≈3), and 20 ppm $H_2C_2O_4$/3 ppm Fe $<>$ 0.158 mM $H_2C_2O_4$/0.054 mM Fe (≈3), respectively. However, when the molar ratio is below 3, insufficient oxalate amount is present, and some of the ferric ions can precipitate as $Fe(OH)_3$, reducing the yield of Fe^{2+} ion regeneration. On the other hand, the efficiency decreased as molar ratio increased $[H_2C_2O_4]$/[Fe] > 3, possibly due to the excess oxalate can not complex with more ferric ions in solution and the light penetration through irradiated wastewater decreases. Besides, the excess of oxalate acts as an additional organic compound and so competes the $^{\bullet}OH$ radicals with the Orange II reducing the decoloration efficiency. This is in agreement with data

Table 3
Saliency analysis of the input variables for the neural network (%)

Neural network output	Parameters					
Decoloration kinetic rate constant, k_d ($W^{-1}\,h^{-1}$)	$[H_2O_2]$	[Fe]	[pH]	[Orange II]	$[H_2C_2O_4]$	[Temperature]
Solar photo-Fenton	21.41	5.70	47.03	12.48	–	13.38
Ferrioxalate-assisted Solar photo-Fenton	26.64	27.07	7.25	–	33.77	5.26

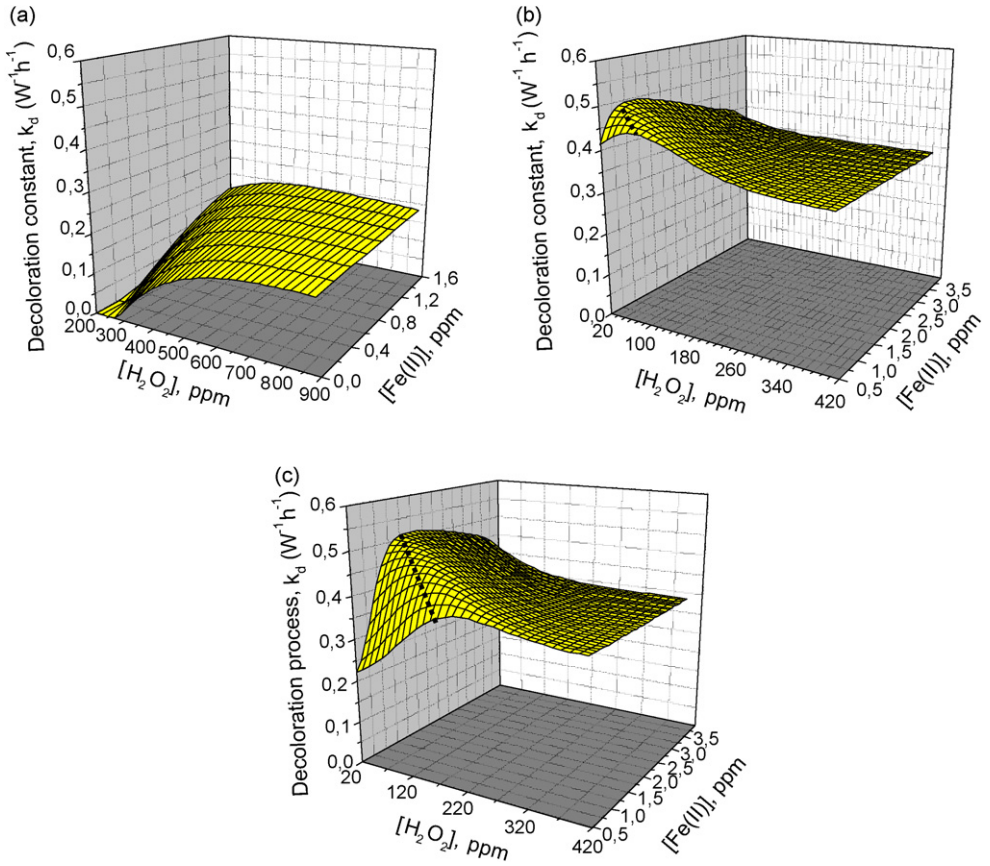

Fig. 4. NNs simulation of the effect of influence of the initial concentration of H_2O_2 and Fe(II) on k_d. (a) Solar photo-Fenton process (pH 3.5, $T = 29$ °C, [OII] = 15 ppm); (b) ferrioxalate-assisted solar photo-Fenton process (pH 3.5, $T = 29$ °C, [OII] = 15 ppm; $[H_2C_2O_4]$ = 10 ppm); (c) ferrioxalate-assisted solar photo-Fenton process (pH 3.5, $T = 29$ °C, [OII] = 15 ppm; $[H_2C_2O_4]$ = 20 ppm).

reported by others authors about degradation of reactive Black B in a photo/ferrioxalate system [43]. On the other hand, the negative effect on the decoloration of dye solution with excess of oxalic acid can be also due to CO_2 produced according to Eq. (3) could be converted to CO_3^{2-} or HCO_3^- at acid pH, which may scavenge the hydroxyl radicals and so to decrease the decoloration efficiency.

Table 4
Reactions and constants for photo-Fenton degradation of Orange II (from reference [39])

No.	Reaction	Rate Constant(l mol^{-1} s^{-1})
1	$Fe^{(II)} + H_2O_2 \rightarrow Fe^{(III)} + {}^{\bullet}OH + OH^-$	63
2	$Fe^{(II)} + {}^{\bullet}OH \rightarrow Fe^{(III)} + OH^-$	3×10^8
3	$H_2O_2 + {}^{\bullet}OH \rightarrow HO_2^{\bullet} + H_2O$	3.3×10^7
4	$Fe^{(II)} + HO_2^{\bullet} \rightarrow Fe^{(III)}(HO_2)^{+2}$	1.2×10^6
5	$HO_2^{\bullet} \rightarrow O_2^{-\bullet} + H^+$	1.58×10^5
6	$O_2^{-\bullet} + H^+ \rightarrow HO_2^{\bullet}$	1×10^{10}
7	$Fe^{(II)} + O_2^{-\bullet} + H^+ \rightarrow Fe^{(III)}(HO_2)^{+2}$	1×10^7
8	$Fe^{(III)} + H_2O \rightarrow Fe^{(III)}(HO_2)^{+2} + H^+$	2×10^{-3}
9	$Fe^{(III)}(HO_2)^{+2} + H^+ \rightarrow Fe^{(III)} + H_2O$	0.645
10	$Fe^{(III)}(HO_2)^{+2} \rightarrow Fe^{(III)} + HO_2^{\bullet}$	2.7×10^{-3}
11	$Fe^{(III)} + HO_2^{\bullet} \rightarrow Fe^{(II)} + O_2 + H^+$	2×10^3
12	$Fe^{(III)} + O_2^{-\bullet} \rightarrow Fe^{(II)} + O_2$	5×10^7
13	$HO_2^{\bullet} + HO_2^{\bullet} \rightarrow H_2O_2 + O_2$	8.3×10^5
14	$HO_2^{\bullet} + O_2^{-\bullet} + H^+ \rightarrow H_2O_2 + O_2$	9.7×10^7
15	${}^{\bullet}OH + HO_2^{\bullet} \rightarrow H_2O + O_2$	7.1×10^{-9}
16	${}^{\bullet}OH + O_2^{-\bullet} \rightarrow OH^- + O_2$	1×10^{10}
17	${}^{\bullet}OH + {}^{\bullet}OH \rightarrow H_2O_2$	5.2×10^9
18	$H_2O_2 + h\upsilon \rightarrow 2\ {}^{\bullet}OH$	–

Fig. 5a and b shows an example of the effect of initial concentrations of oxalic acid and ferrous ion on hydrogen peroxide remaining in solution for this process. We can see in Fig. 5a (initial conditions: [Fe(II)] = 2 ppm), $[H_2O_2]$ = 225 ppm, [Orange II] = 15 ppm, pH 3.5, $T = 29$ °C) that at a low initial concentration of Fe(II) (2 ppm), the amount of H_2O_2 remaining in solution is always higher with increasing initial oxalic acid concentration showing that hydrogen peroxide is in excess causing the above mentioned scavenger effect.

On the other hand, Fig. 5b (initial conditions: $[H_2O_2]$ = 225 ppm, [Orange II] = 15 ppm, [oxalic] = 30 ppm, pH 3.5, $T = 29$ °C) shows that an increase in the initial Fe(II) concentration leads to a decrease of the amount of H_2O_2 remaining in solution since hydrogen peroxide is consumed more rapidly by reaction with Fe^{2+} ions, light "$h\upsilon$" and a higher amount of ${}^{\bullet}OH$ radicals produced.

3.1.2. Effect of pH

pH is an important parameter for photo-Fenton processes. It affects the generation of hydroxyl radicals and the nature of iron species in solution. The results showed that Orange II photo-degradation should depend strongly on the pH value in the SPF system (pH range: 2–8) but its influence is insignificant in the SPFox system due to the small range of pH studied (pH range:

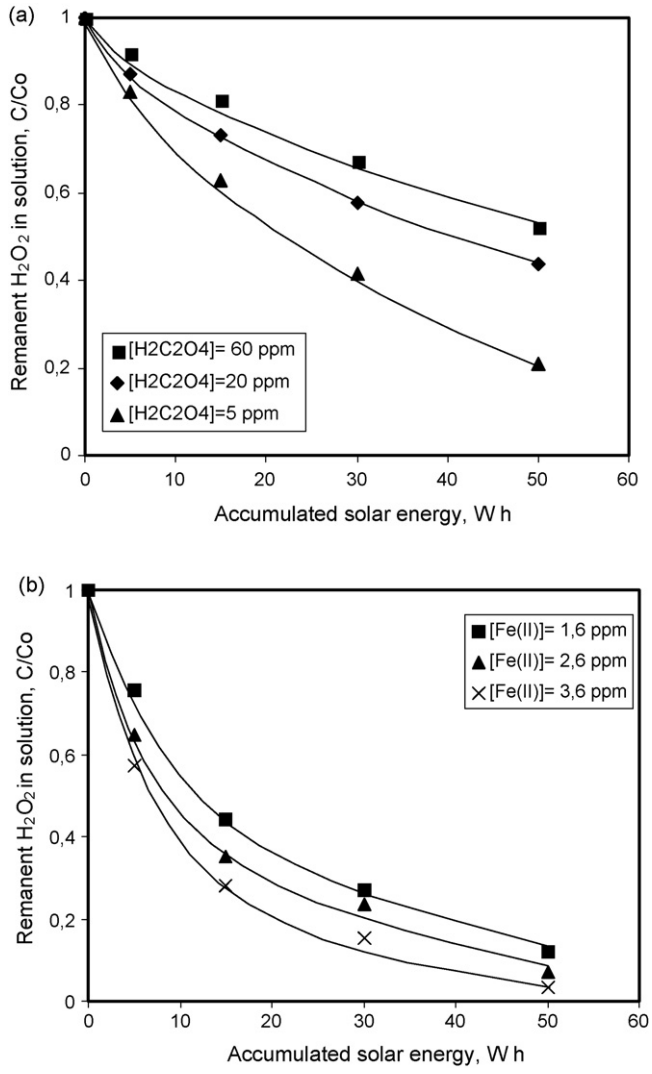

Fig. 5. Effect of initial oxalic and Fe(II) concentrations on H_2O_2 residual. (a) pH 3.5; $[H_2O_2]$ = 225 ppm; [Orange II] = 15 ppm; [Fe(II)] = 2 ppm; T = 29 °C. (b) pH 3.5; $[H_2O_2]$ = 225 ppm; [Orange II] = 15 ppm; $[H_2C_2O_4]$ = 30 ppm; T = 29 °C.

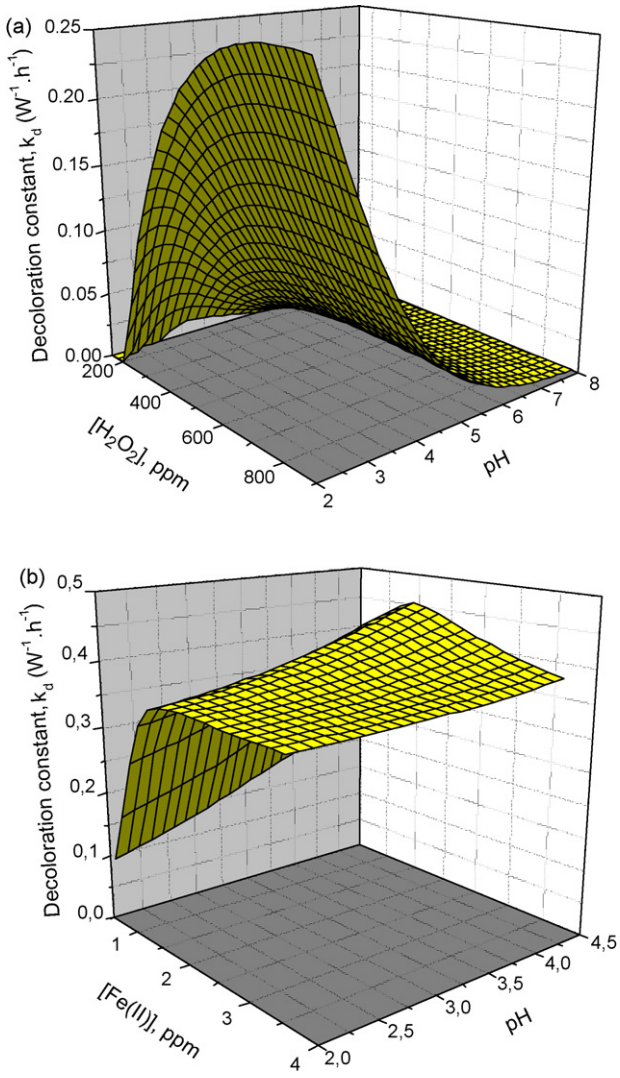

Fig. 6. Effect of pH on dye decoloration rate. (a) SPF system; [Orange II] = 15 ppm; [Fe(II) = 3 ppm; T = 29 °C; (b) SPFox system; $[H_2O_2]$ = 300 ppm; [Orange II] = 15 ppm; $[H_2C_2O_4]$ = 15 ppm; T = 29 °C.

2–4.5) as shown in Table 3. The influence of pH on decoloration of Orange II is also shown in Fig. 6. In the SPF system (Fig. 6a), the maximum decoloration constant was k_d 0.23 W^{-1} h^{-1} at pHs 2–3. Above pH 3, the decrease in decoloration constant is due to the reduction of the Fe^{2+} catalysis to decompose H_2O_2 by the coagulation of Fe^{3+} complex formed in the reaction [44].

When the pH value increases up to 6, the Fe^{3+} and Fe^{2+} species cannot almost exist in the wastewater and the predominant specie of Fe was $Fe(OH)_3$ as the precipitate, which might hardly be photoactive and cannot be regenerated to the ferrous ion, in agreement with other authors [45].

In the SPFox system (Fig. 6b), pH 4.5 was found to be the optimum pH to degrade Orange II. This is an important advantage because it allows using less acid to acidify the medium and reduce the operation costs. These results are in agreement with previous studies which have reported that when pH is lower than 5, the main Fe(III) species are $[Fe(C_2O_4)_2]^-$ and $[Fe(C_2O_4)_3]^{3-}$ which are highly photoactive [45,46] and under solar UV light they can effectively convert Fe^{3+} ion into Fe^{2+} ion by the Eq. (1), being more hydroxyl radicals generated by reaction of generated ferrous ions with hydrogen peroxide. Besides, $[Fe(C_2O_4)_3]^{3-}$ can also produce H_2O_2 under UV light irradiation as it is indicated in Eqs. (1)–(5). Thus, the addition of oxalic acid to degrade the Orange II solution can not only improve the degradation reaction, but oxalic acid may also be used to adjust the pH of dye solution and reduce the operation costs.

3.1.3. Effect of temperature and initial dye concentration

As can be expected, when the temperature of the reaction medium was increased (range studied: 20–29 °C), decoloration proceeds at a faster rate due to the exponential dependence of the kinetic constants on it (Arrhenius law). The increase of initial dye concentration decreases the probability of reaction between dye molecules and the hydroxyl radicals generated in the reaction medium (constant

value for the same conditions of H_2O_2, Fe and oxalic) reducing the decoloration efficiency. Besides, at high initial dye concentrations, the path length of photon entering into the solution decreases and the amount of hydroxyl radicals generated decreases.

3.2. Mineralization under the optimum conditions. A comparative study

In order to determine the extent of mineralization of Orange II, TOC value of the solution was measured during the photodegradation. As previously reported [41], the addition of H_2O_2 to OII solutions under artificial UV light or sunlight in the absence of catalyst did not lead to significant mineralization due to the $^{\bullet}OH$ radicals generated by the reaction without catalyst is not enough. Therefore, the presence of an effective catalyst such us Fe is necessary for the mineralization of Orange II.

A long experiment monitoring TOC, COD, color and H_2O_2 in solution was made under optimum conditions selected from NNs for the two processes studied, SPF and SPFox systems: SPF process: ($[H_2O_2]$ = 450 ppm, [Fe(II)] = 1.6 ppm, [Orange II] = 25 ppm, pH 3) and SPFox process: ($[H_2O_2]$ = 120 ppm, [Fe(II)] = 2 ppm, [Orange II] = 25 ppm, pH 3.25, $[H_2C_2O_4]$ = 13.3 ppm). Results in Fig. 7 show that, in both systems, at the beginning of the reaction when a low radical concentration has been generated, these radicals preferentially attack and breakdown the azo double bond (N=N) in the chromophore group. Hundred percent of dye solution decoloration was obtained in both systems but with different accumulated solar energy and so different reaction times (SPF: 34 W h, 45 min; SPFox: 16 W h, 15 min).

In a second stage, $^{\bullet}OH$ radicals attack the benzene and naphtalene rings of OII molecule. Analysis of the UV–vis absorption spectra of Orange II (data not shown) before and after oxidation allows to conclude that naphthalene ring is broken sooner than benzene ring). Fig. 7 shows that 150 ppm and 112 ppm of H_2O_2 were necessary to complete decoloration of 25 ppm of Orange II by the SPF and SPFox systems. In that moment, 10% TOC and 7% COD removal (SPF system) and 50% TOC and 10% COD removal (SPFox system) have been achieved. However, 80% and 100% COD removal is attained after 210 min of oxidation (≈200 W h) in SPF and SPFox systems, respectively. It must be remarked that in the SPFox process, when H_2O_2 in solution disappeared, the TOC reduction ceased (70% TOC removal). An additional test adding 120 ppm of H_2O_2 to the solution after complete decoloration of the dye under the SPFox system (data not shown) lead to COD total reduction and 80% TOC removal in 180 min. TOC reduction is due to the decarboxylation of organic-acid intermediates [47]:

$$[Fe^{(III)}(RCO_2)^-]^{+2} + h\nu\, Fe^{(II)} + CO_2 + R^{\bullet} \quad (9)$$

Based on our results of dye degradation by the ferrioxalate-assisted solar photo-Fenton process, the following stoichiometry for the mineralization of Orange II could be suggested,

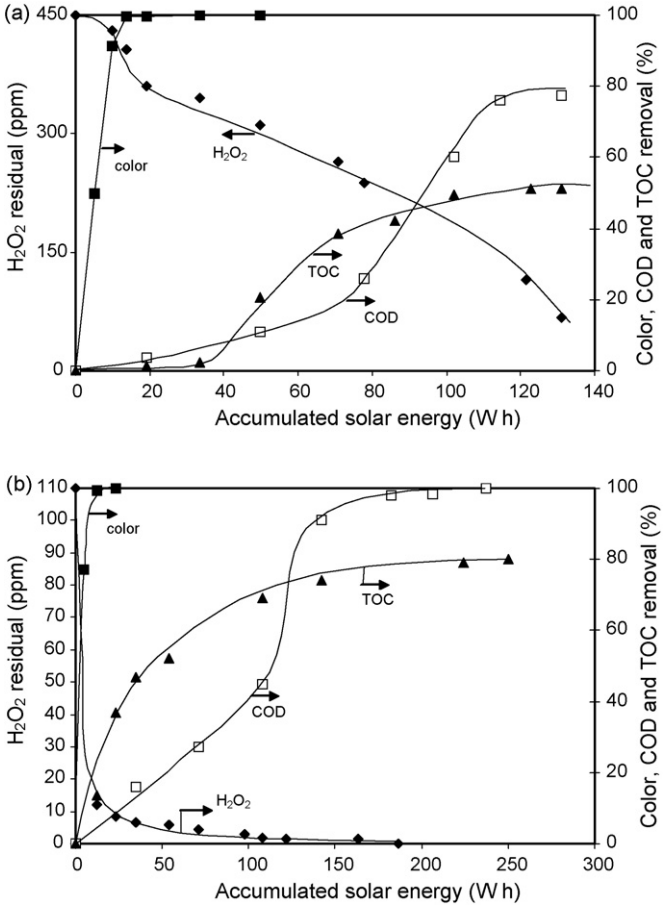

Fig. 7. Evolution of color, TOC, COD and H_2O_2 in solution under the optimum conditions for the two processes: (a) SPF system ($[H_2O_2]$ = 450 ppm, [Fe(II)] = 1.6 ppm, [Orange II] = 25 ppm, pH 3); (b) SPFox system ($[H_2O_2]$ = 120 ppm, [Fe(II)] = 2 ppm, [Orange II] = 25 ppm, pH 3.25, $[H_2C_2O_4]$ = 13.3 ppm).

taking also into account the above mentioned equations, mainly Eqs. (1) and (8)–(12) shown in Table 4.

$$C_{16}H_{11}N_2NaO_4S + 42H_2O_2 \rightarrow 16CO_2 + 46H_2O + 2HNO_3 + NaHSO_4$$

On the basis of this equation, 42 mol of H_2O_2 are theoretically needed to completely degrade 1 mol of Orange II, which produces 2 moles of HNO_3 and 1 mol of $NaHSO_4$. In our case, 110 ppm H_2O_2 are required to complete degradation of 25 ppm Orange II, optimal ratio $[H_2O_2]$/[Orange II] equals 45, that is only slightly higher than the theoretical value. On the other hand, according to Eq. (10), the mineralization of 25 ppm of Orange II produces 8.99 ppm nitrate and 5.71 ppm sulphate. In our case, 7.2 ppm nitrate and 4.5 ppm sulphate were obtained, that is in agreement with the 80% TOC removal achieved.

It is important to point out that these results were obtained using 2 ppm of ferrous ion (discharge legal limit), which reduces the process costs since the removal of Fe ions at the end of treatment would not be necessary.

4. Conclusions

Degradation of Orange II solutions was developed in a compound parabolic collector (which allows a continuous treatment of waste water being an industrially feasible technique) under solar photo-Fenton and ferrioxalate-assisted solar photo-Fenton systems using ferrous initiated processes. The use of ferrous sulphate is advantageous since it is less corrosive than ferric salts, very cheap and more soluble than ferric compounds.

A comparative study of these two systems was done by using multivariate experimental design and neural networks fitting.

Hundred percent decoloration of dye solution can be reached by using both processes, but with different irradiation times. However, the efficiency of TOC and COD removal was higher in the SPFox process since ferrioxalate complexes absorb strongly and a higher portion of the solar spectrum can be used. In addition, the solar photo-Fenton degradation with oxalic acid is efficient and permits the use of a concentration of Fe (2 ppm) below discharge criterion according to European Union and besides, oxalic acid can be used to pH adjustment, reducing the operation costs of Fe removal and chemicals.

Acknowledgement

Financial support from the Programa de Ciencias y Tecnologías Químicas (Junta de Comunidades de Castilla-La Mancha, Spain, (PAI06-0050-2582) is gratefully acknowledged.

References

[1] I. Arslan, I.A. Balcioglou, Dyes Pigments 43 (1999) 95–108.
[2] F.P. Van der Zee, G. Lettinga, J.A. Field, Chemosphere 44 (2001) 1169–1176.
[3] M. Rodríguez, S. Malato, C. Pulgarín, S. Contreras, D. Curcó, J. Giménez, S. Esplugas, Solar Energy 79 (2005) 360–368.
[4] T. Robinson, G. McMullan, R. Marchant, P. Nigam, Biores. Technol. 77 (2001) 247–255.
[5] C. Galindo, P. Jacques, A. Kalt, Chemosphere 45 (2001) 997–1005.
[6] R.F.P. Nogueira, M.R.A. Silva, A.G. Trovó, Solar Energy 79 (2005) 384–392.
[7] J. Feng, X. Hu, P.L. Yue, H.Y. Zhu, G.Q. Lu, Water Res. 37 (2003) 3776–3784.
[8] J. Pignatello, Environ. Sci. Technol. 26 (1992) 944–951.
[9] M. Pérez, F. Torrades, X. Domenech, J. Peral. Water Res. 36 (2002) 2703–2710.
[10] S. Malato, J. Blanco, A. Vidal, C. Richter, Appl. Catal. B: Environ. 37 (2002) 1–15.
[11] M. Swaminathan, M. Muruganandham, Solar Energy Mater. Solar Cells 81 (2003) 439–457.
[12] I.K. Konstantinou, T.A. Albanis, Appl. Catal. B: Environ. 49 (2004) 1–14.
[13] D. Robert, A. Piscopo, J.V. Weber, Solar Energy 77 (2004) 553–558.
[14] D. Gumy, P. Fernández-Ibañez, S. Malato, C. Pulgarín, O. Enea, J. Kiwi, Catal. Today 101 (2005) 375–382.
[15] P.L. Huston, J.J. Pignatello, Water Res. 33 (1999) 1238–1246.
[16] R.F.P. Nogueira, J.R. Guimaräes, Water Res. 34 (2000) 895–901.
[17] C.A. Emilio, W.F. Jardim, M.L. Litter, H.D. Mansilla, J. Photochem. Photobiol. A 151 (2002) 121–127.
[18] G.D. Copper, G.D. DeGraff, J. Phys. Chem. 76 (1972) 2618–2625.
[19] D.L. Sedlak, J. Hoigné, Atmos. Environ. 27 (1993) 2173–2185.
[20] Y.G. Zuo, Geochim. Cosmochim. Acta 59 (1995) 3123–3130.
[21] K. Selvam, M. Muruganandham, M. Swaminathan, Solar Energy Mater. Solar Cells 89 (2005) 61–74.
[22] N. Daneshvar, H. Ashassi-Sorkhabi, A. Tizpar, Sep. Purif. Technol. 31 (2003) 153–162.
[23] J. Bandara, C. Morrison, J. Kiwi, C. Pulgarín, P. Peringer, J. Photochem. Photobiol. A Chem. 99 (1996) 57–66.
[24] J. Kiwi, M.R. Dhananjeyan, J. Albers, O. Enea, Helv. Chim. Acta 84 (2001) 3433–3445.
[25] X. Hu, J. Feng, P.L. Yue, Environ. Sci. Technol. 38 (2004) 269–275.
[26] J. Chen, L. Zhu, J. Photochem. Photobiol. A Chem. 188 (2007) 56–64.
[27] J. Herney Ramirez, C.A. Costa, L.M. Madeira, G. Mata, M.A. Vicente, M.L. Rojas-Cervantes, A.J. López-Peinado, R.M. Martín-Aranda, Appl. Catal. B: Environ. 71 (2007) 44–56.
[28] L.M. Madeira, J.H. Ramirez, F.J. Maldonado-Hódar, A.F. Pérez-Cadenas, C. Moreno-Castilla, C.A. Costa, Appl. Catal. B: Environ. 75 (2007) 317–328.
[29] X. Hu, J. Feng, P.L. Yue, H.Y. Zhu, G.Q. Lu, Ind. Eng. Chem. Res. 42 (2003) 2058–2066.
[30] H.Q. Yu, Y. Mu, S.J. Zhang, J.C. Zheng, J. Chem. Technol. Biotechnol. 79 (2004) 1429–1431.
[31] W. Feng, D. Nansheng, H. Helin, Chemosphere 41 (2000) 1233–1238.
[32] H.D. Mansilla, J. Fernández, J. Kiwi, J. Baeza, J. Freer, C. Lizama, Appl. Catal. B Environ. 48 (2004) 205–211.
[33] M.B. Ray, A. Bhattacharya, S. Kawi, Catal. Today 98 (2004) 431–439.
[34] M.B. Ray, G. Li, X.S. Zhao, Sep. Purif. Technol. 55 (2007) 91–97.
[35] V. Augugliaro, C. Baiocchi, A.B. Prevot, M.C. Brussinno, E. García-López, V. Loddo, S. Malato-Rodriguez, G. Marci, L. Palmisano, M. Pazzi, E. Pramauro, Chemosphere 49 (2002) 1223–1230.
[36] G.E.P. Box, W.G. Hunter, J.S. Hunter, Statistics for experimenters: an introduction to design, data analysis and model building, Ed. Wiley, New York, 1978.
[37] D.P. Morgan, C.L. Scofield, Neural Networks and Speech Processing, Kluwver Academic Publishers, London, 1991.
[38] R. Nath, B. Rajagopalan, R. Ryker, Comput. Oper. Res. 24 (1997) 767–773.
[39] A. Durán, J.M. Monteagudo, M. Mohedano, Appl. Catal. B: Environ. 65 (2006) 127–134.
[40] A. Durán, J.M. Monteagudo, E. Amores, Appl. Catal. B: Environ. 80 (2008) 42–50.
[41] J.M. Monteagudo, A. Durán, Chemosphere 65 (2006) 1242–1248.
[42] S. Sabhi, J. Kiwi, Water Res. 35 (2001) 1994–2002.
[43] Y.H. Huang, S.T. Tsai, Y.F. Huang, C.Y. Chen, J. Hazard. Mater. 140 (2007) 382–388.
[44] H. Zheng, Y. Pan, X. Xiang, J. Hazard. Mater. 141 (2007) 457–464.
[45] F.B. Li, X.Z. Li, X.M. Li, T.X. Liu, J. Dong, J. Colloid Inter. Sci. 311 (2007) 481–490.
[46] M.E. Balmer, B. Sulzberger, Environ. Sci. Technol. 30 (1999) 2418–2424.
[47] J.G. Sagawe, A. Lehnard, M. Lübber, D. Bahnemann, Helv. Chim. Acta 84 (2001) 3742–3759.